




Article

The Sonocatalytic Activation of Persulfates on Iron Nanoparticle Decorated Zeolite for the Degradation of 1,4-Dioxane in Aquatic Environments

Surya Teja Malkapuram ¹, Shirish Hari Sonawane ^{1,2,*} , Manoj P. Rayaroth ^{3,4} , Murali Mohan Seepana ¹, Sivakumar Manickam ⁵, Jakub Karczewski ⁶ and Grzegorz Boczkaj ^{4,*} 

¹ Department of Chemical Engineering, National Institute of Technology Warangal, Warangal 506004, India; ms720069@student.nitw.ac.in (S.T.M.); murali@nitw.ac.in (M.M.S.)

² Department of Process Engineering and Chemical Technology, Faculty of Chemistry, Gdansk University of Technology, G. Narutowicza St. 11/12, 80-233 Gdansk, Poland

³ GREMI, UMR 7344, CNRS, Université d'Orléans, 45067 Orléans, France; manoj.pr024@gmail.com

⁴ Department of Sanitary Engineering, Faculty of Civil and Environmental Engineering, Gdansk University of Technology, G. Narutowicza St. 11/12, 80-233 Gdansk, Poland

⁵ Petroleum and Chemical Engineering Faculty of Engineering, Universiti Teknologi Brunei, Bandar Seri Begawan BE1410, Brunei; manickam.sivakumar@utb.edu.bn

⁶ Department of Solid State Physics, Faculty of Applied Physics and Mathematics, Gdańsk University of Technology, Narutowicza Street 11/12, 80-233 Gdansk, Poland; jakub.karczewski@pg.edu.pl

* Correspondence: shirish@nitw.ac.in (S.H.S.); grzegorz.boczkaj@pg.edu.pl (G.B.)

Abstract: In the chemical industry, 1,4-diethylene dioxide, commonly called dioxane, is widely used as a solvent as well as a stabilizing agent for chlorinated solvents. Due to its high miscibility, dioxane is a ubiquitous water contaminant. This study investigates the effectiveness of catalyst- and ultrasound (US)-assisted persulfate (PS) activation with regard to degrading dioxane. As a first step, a composite catalyst was prepared using zeolite. A sonochemical dispersion and reduction method was used to dope zeolite with iron nanoparticles (FeNP/Z). In the subsequent study, the reaction kinetics of dioxane degradation following the single-stage and two-stage addition of PS was examined in the presence of a catalyst. Using GC-MS analysis, intermediate compounds formed from dioxane degradation were identified, and plausible reaction pathways were described. Upon 120 min of sonication in the presence of a catalyst with a two-stage injection of PS, 95% 100 mg/L dioxane was degraded. Finally, the estimated cost of treatment is also reported in this study. Sonolytically activated PS combined with a FeNP/Z catalyst synergizes the remediation of biorefractory micropollutants such as dioxane.

Keywords: emerging organic pollutants; advanced oxidation processes (AOPs); wastewater treatment; composite catalyst; nanomaterials



Citation: Malkapuram, S.T.; Sonawane, S.H.; Rayaroth, M.P.; Seepana, M.M.; Manickam, S.; Karczewski, J.; Boczkaj, G. The Sonocatalytic Activation of Persulfates on Iron Nanoparticle Decorated Zeolite for the Degradation of 1,4-Dioxane in Aquatic Environments. *Catalysts* **2023**, *13*, 1065. <https://doi.org/10.3390/catal13071065>

Academic Editors: Slimane Merouani and Antonio Eduardo Palomares

Received: 4 May 2023

Revised: 27 June 2023

Accepted: 28 June 2023

Published: 1 July 2023



Copyright: © 2023 by the authors. Licensee MDPI, Basel, Switzerland. This article is an open access article distributed under the terms and conditions of the Creative Commons Attribution (CC BY) license (<https://creativecommons.org/licenses/by/4.0/>).

1. Introduction

Exponential demand for new kinds of materials has led to the development of emerging pollutants that have been categorized as contaminants of emerging concern (CEC), meaning that they can adversely affect human, animal, and environmental health even at lower concentrations [1–4]. The following pollutants are examples of CECs: pharmaceuticals and personal care products (PPCPs), flame retardants, endocrine-disrupting compounds (EDCs), fertilizers, pesticides, herbicides, artificial sweeteners, polyaromatic hydrocarbons, etc. The presence of CECs is extremely dangerous, and the removal of these pollutants from aquatic environments is also a herculean task [5,6]. Due to their point and non-point sources, these pollutants are often present in water bodies and degrade the water quality to unacceptable levels [7]. A cyclic ether belonging to the CEC class is 1,4-diethylene dioxide (C₄H₈O₂). It is popularly known as dioxane and 1,4-dioxane. It is used for various

industrial applications, including as a solvent, a wetting agent, a dispersing agent, and a solvent stabilizer for chlorinated substances [8,9]. It is also used for the production of dyes, paper, adhesives, etc. [10]. As a by-product from the production of ethoxylated-based surfactants, it is also found as a trace element in personal care products [11]. It is highly soluble in polar compounds. As a result of its high solubility in water (431×10^3 mg/L) [12], it is stable in aquatic environments and causes adverse effects [13]. Despite its low concentrations (μg), dioxane is a carcinogen and, according to the International Agency for Research on Cancer, is categorized as a group B2 carcinogen [12]. Additionally, exposure to dioxane causes irritation to the respiratory tract and eyes, and it can severely cause damage to the liver, central nervous system, and kidneys [14]. Further, the pollutant is resistant to most of the classical wastewater treatment (WWT) methods, including biological processes. This is because of its heterocyclic ether bonds, high miscibility, low vapor pressure, and low boiling point. Hence, its presence is persistent in drinking water, sewage water, ground water, and surface water [10].

Conventional treatment processes, such as chemical precipitation and the activated sludge process, cannot remove dioxane completely; thus, it is present in treated water. Disinfection methods based on Chlorine can produce several by-products, such as trihalomethanes and haloacetic acids, which can cause cancer and affect reproduction. Further, dioxane is biorecalcitrant towards biological methods as its presence inhibits microbial growth. Thus, there is a need for more effective treatment methods.

In recent times, advanced oxidation processes (AOPs) have gained huge attention due to the in situ generation of oxidizing radicals, especially hydroxyl radicals ($\bullet\text{OH}$) and sulfate ($\text{SO}_4^{\bullet-}$), which are non-selective towards pollutants present in the water/wastewater [14–16]. The generation of radicals can be achieved through (1) energy sources such as ultrasound (US), electricity, and ultraviolet rays, (2) oxidizing agents like peroxide, persulfate (PS), ozone, and oxygen, or (3) with the help of catalysts and (4) by combining the aforementioned factors [17]. The generated radicals attack pollutants present in the aquatic environment and oxidize them to create simpler organic compounds. It is proven that the complete mineralization of organic compounds into carbon dioxide and water is possible in the best scenario [14]. Extensive studies have been conducted on the photocatalytic and electrochemical degradation of various pollutants; however, due to their limitations, such as catalyst cost, catalyst loss, recombination of proton–electron pairs, volatilization of pollutants, generation of toxic molecules, incomplete destruction of pollutants, electrode erosion, etc., their implementation at actual treatment plants has been hindered [18,19]. The electrooxidation of dioxane present in simulated plate industry water was able to remove 85.4% dioxane. However, it has been identified that degradation results in toxic byproducts and electrode fouling. Additionally, degradation requires high-energy input [20]. Likewise, photocatalysis also results in the highly efficient removal of dioxane (~70%) from water; however, catalyst deactivation, the generation of toxic byproducts, and issues related to catalyst recovery limit its implementation [21].

Recently, cavitation technologies, particularly ultrasounds, have been proven to be very effective for water and wastewater treatment. Ultrasound (US) technology is clean, cheap, effective, and green. Regarding the use of US technology, an acoustic wave is used to induce the cavitation phenomena in the liquid medium to remediate the pollutants present in the water. The propagation of waves in a high-frequency liquid creates voids (bubbles) in the water due to variations in local pressure. Due to the oscillating nature of sound wave, there always exists pressure variations that cause bubbles to grow and implode continuously. The implosion of bubbles results in localized and intense shock waves, microjets, and radical generation [22].

They are widely employed to eliminate various pollutants, including pharmaceuticals, pesticides, microorganisms, dyes, alcohols, and phenolic compounds [23,24]. Xu et al. (2012) [25] examined the combined effect of ozonation and US on dioxane degradation. A combination of ozone microbubbles and US technology has increased hydroxyl radicals due to the ozone sonolysis process. Several US studies have been conducted on different

combinations of catalysts, photocatalysts, molecular sieves, oxidants, etc., to treat water and wastewater [26].

Lately, PS has received increased attention in wastewater treatment technologies due to its dual action involving radicals and electron transfer processes. It is widely used to remove many pollutants from water environments [27,28]. Moreover, PS' lifespan in groundwater is much shorter than other oxidants, such as ozone and peroxide. From a cost perspective, PS is also less expensive [29]. PS has subsequently been employed in several US studies to enhance pollutant degradation. PS is activated by the temperature generated by sonolysis [26]. Subsequently, the combination has gained attention for its potential use in degrading dyes and other pollutants. For example, PS activated by the sonochemical method has been used to degrade 1,1,1-trichloroethane, dyes, aromatic compounds, coal tar, nitrobenzene, and other CECs. Furthermore, it is used to mineralize organic pollutants [26,30].

In recent times, the utilization of catalysts in AOPs for converting highly oxidizing radicals into reactive oxygen species (ROS) has been widely studied. The presence of catalysts triggers the activation of oxidizing radicals, which in turn can easily attack various kinds of pollutants and break their bonds to degrade into harmless compounds. The presence of catalysts in AOPs also increases the degradation rate, thus reducing the operation time [31]. Furthermore, it is evident that heterogeneous catalysts can provide vastly superior performance than homogeneous catalysts, especially for the activation of permonoxysulfates (PMS) [32]. Henceforth, a great amount of research is being carried out in order to fabricate suitable heterogeneous catalysts for the effective degradation of organic pollutants using AOP technology.

As an adsorbent, a catalyst, and a filter, molecular sieves, a class of zeolites, are widely used in wastewater treatment processes [33,34]. They are usually doped with various elements to improve their physical and chemical properties. In addition, US studies have included doped molecular sieves to improve the kinetics of degradation. As a result of the synergistic effect of the US in conjunction with molecular sieves, a wide range of research is currently being conducted on this topic [35]. The doping of materials with transition metals such as iron nanoparticles (FeNPs) can effectively modify the structure of the material. Iron is abundantly available in the environment and non-toxic in nature; thus, the immobilization of FeNPs on zeolite can reduce the catalyst's cost and provide much greener solutions [36].

This study used a sonochemical method to impregnate molecular sieves with FeNPs. Initially, sonolytically activated PS was investigated for its ability to degrade dioxane. Firstly, for the dioxane degradation studies, the adsorbent nature of FeNP/Z was tested. Later, the combined effect of the sonolytically activated PS in the presence of a FeNP-decorated zeolite (FeNP/Z) catalyst was examined. This study optimized parameters such as the operation time and amount of PS and catalysts for the degradation of dioxane. Additionally, the reaction kinetics were developed using rate laws, and plausible degradation pathways were derived from GC-MS analyses of the intermediates formed from the degradation of dioxane. Furthermore, the cost estimation per 1 m³ of wastewater treatment is also estimated in this paper. This novel approach to dioxane degradation, which includes using sonolytically activated PS in the presence of a FeNP/Z catalyst, provides a good basis for future studies on the degradation of other CECs.

2. Results and Discussion

2.1. Characterization of Catalyst

To confirm the impregnation of FeNPs, various characterization tests were carried out. To identify its crystallographic structure, X-ray Diffraction (XRD) was performed. It is believed that the activity of US technology tears the clusters of FeNPs, thus avoiding the agglomeration of particles and enhancing the dispersion onto the zeolite matrix. As shown in Figure 1, the XRD patterns indicated that FeNPs was impregnated on zeolite. The peaks at 2θ values of 30.4° and 34.7° represent the presence of iron compounds in the



zeolite matrix [37]. However, due to the adjustment of FeNPs in the zeolite matrix, peaks slightly shifted away from pure zeolite 2θ location. The adjustment of FeNPs on zeolite thus provided the composite catalyst with an amorphous character. However, this does not affect the structure of zeolite. Similar results have been reported in studies conducted by Cirlene et al. (2015) [38].

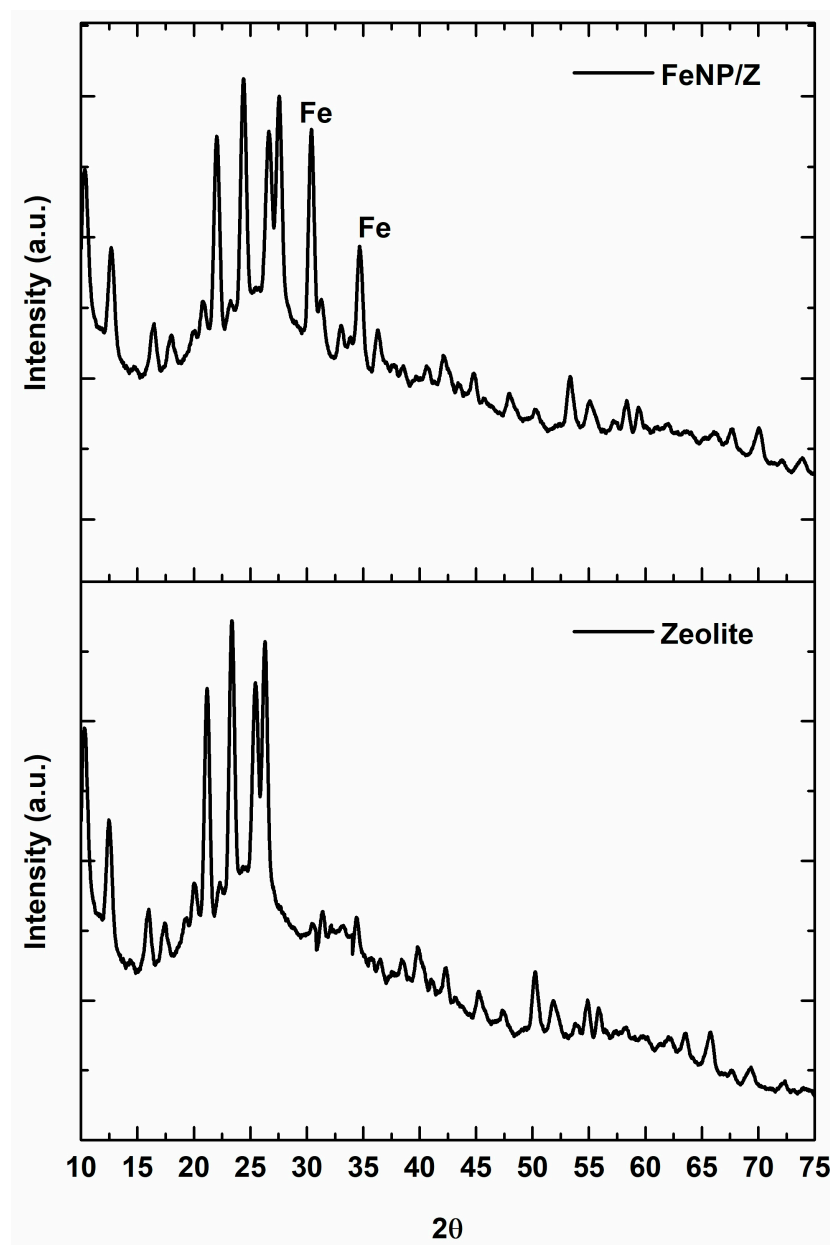


Figure 1. XRD patterns of iron impregnated molecular sieve.

As shown in Figure 2, the scanning electron microscopy (SEM) image of the composite catalyst reveals clusters of small particles stretching over a two-dimensional (2D) crystal structure. The clusters of small-scale particles are believed to be FeNPs on the surface of the zeolite (crystal structure), as reported in the literature [39]. Energy-dispersive X-ray Spectroscopy (EDS) was used to determine the elemental composition of the catalyst. In the study (Figure 3), FeNPs were used to modify the surface of zeolite as the weight percentage of Fe particles increased from 2.97% to 5.92% of the actual composition of the zeolite.

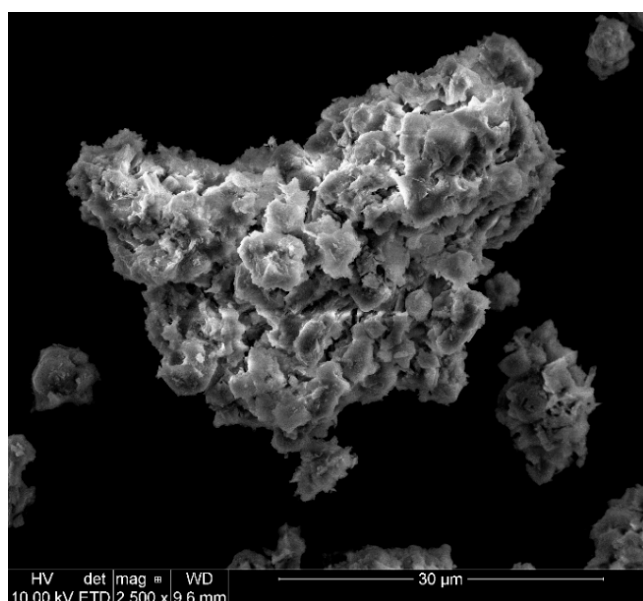


Figure 2. SEM analysis of the surface morphology of FeNP/Z.

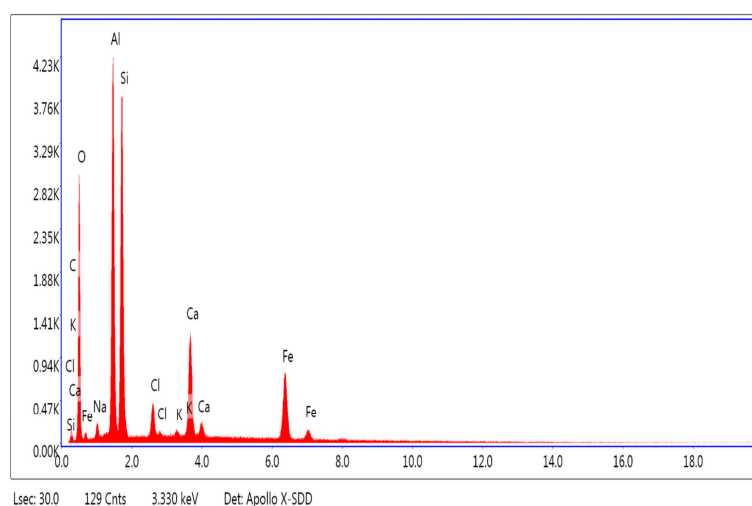


Figure 3. Elemental analysis of FeNP/Z using EDS.

Even though, the metal nanoparticles with zero valence cannot be determined via X-ray Photoelectron Spectroscopy (XPS), the analysis was carried out to identify the possibility of FeNP oxidation. According to the XPS spectra in Figure 4, Fe 2p_{3/2} and Fe 2p_{1/2} stretched around 711 eV and 725 eV, respectively. This confirms the oxidation of FeNPs into their Fe²⁺ and Fe³⁺ oxidation states at 710.3 eV and 712.1 eV, respectively [40]. The atomic weight percentages of Fe²⁺ and Fe³⁺ in the zeolite matrix were 0.43% and 1.4%, respectively. This is in alignment with studies pertaining to Fe doping on graphene [41] and FeNP-embedded carbon nanotubes [40]. Thus, under the influence of US technology, the presence of Fe²⁺ and Fe³⁺ facilitates Fenton-like reactions and activates persulfate (S₂O₈²⁻) to form sulfate radicals (SO₄^{•-}), which are responsible for the degradation of dioxane [42].

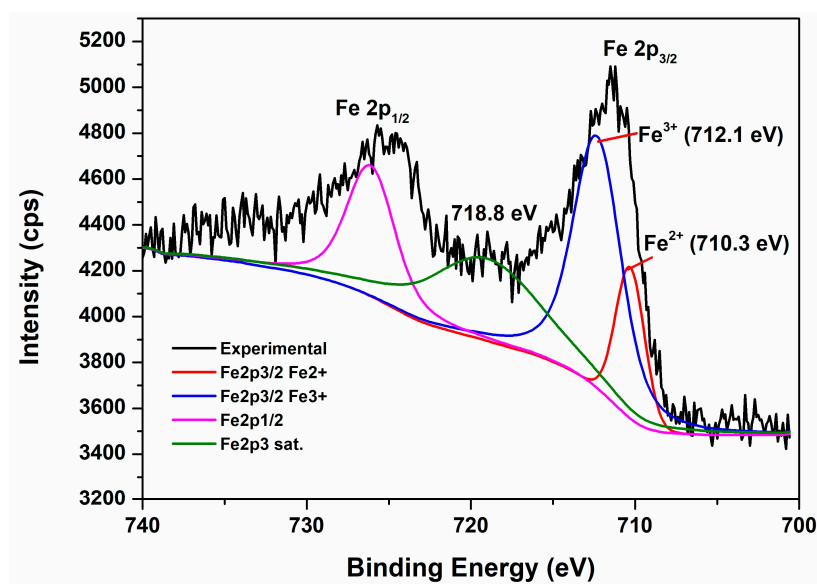


Figure 4. XPS spectrum of synthesized composite catalyst for the identification of oxidized forms of iron.

2.2. Effect of Persulfate and Catalyst on Dioxane Degradation

Dioxane degradation experiments were conducted as described in Section 3.2.2. Firstly, the adsorption tests of FeNP/Z were performed to examine its effectiveness in terms of dioxane removal. A 5 mg catalyst was used in 100 ppm dioxane solution and observed for 2 h. It was found that adsorption for resulted in only 4% of dioxane being removed from the solution. This is likely because the adsorption of dioxane onto an adsorbent is quite slow and/or because the composite is not suitable for the adsorption of dioxane. Further, it may require a greater quantity of adsorbent, which is not economically feasible [42,43]. Later, the behavior of FeNP/Z was studied in the presence of PS and US separately. Even though there was an increment increase in the levels of dioxane removal, 8% for PS and 13% for US, the extent of these increases were considered quite unsatisfactory.

For the sonocatalytic activation of PS, at first, only the effect of acoustic cavitation on dioxane degradation was examined. A later test examined the effect of activating persulfate using US technology and its impact on dioxane degradation. Even though the oxidant-to-pollutant molar ratio ($R_{ox} = 4$) was optimal in our previous studies, wherein the effects of PS on dioxane degradation are discussed [44], the current tests were conducted with an oxidant-to-pollutant molar ratio (R_{ox}) of 2. Approximately 40% of the degradation efficiency was achieved under these sonochemical conditions due to the evolution of sulfate radical anions. Similar results were reported by Zhu et al. in 2018 [8]. When an US is propagated through the reaction mixture, it activates the PS by breaking O–O bonding and generates sulfate radicals. Thus, it leads to the degradation of contaminant [30]. However, it is believed that the lower R_{ox} could not provide enough radicals to degrade the dioxane. Furthermore, due to the high miscibility of dioxane, the mass transport of dioxane molecules from liquid phase to vapor phase was unsatisfactory, resulting in a decreased influence of cavitation on pollutant degradation.

Moreover, 5 mg FeNP/Z was used as a catalyst to reduce the quantity of oxidants and to enhance pollutant degradation. Subsequently, a comparison was made between the effect of the catalyst and PS on the degradation of dioxane in a sonocavitational reactor. Although the addition of PS to the US reactor enhanced the degradation process, Figure 5 illustrates that combining the catalyst with US and PS led to more pollutant degradation (nearly 70%) than just the combination of US and PS. This may be due to the surface area provided by the catalyst, which consequently resulted in fruitful interactions between oxidizing radicals and pollutants. In addition, the presence of heterogeneous catalysts enhances the rate of cavitation due to the incidence of nuclei of gas in the fissures of the catalysts [45]. Thus,

the improved cavitation rates enhanced pollutant degradation. Additionally, cavitation also results in the breakdown of the catalyst. Consequently, a greater surface area will be available, allowing the reactants to interact with each other.

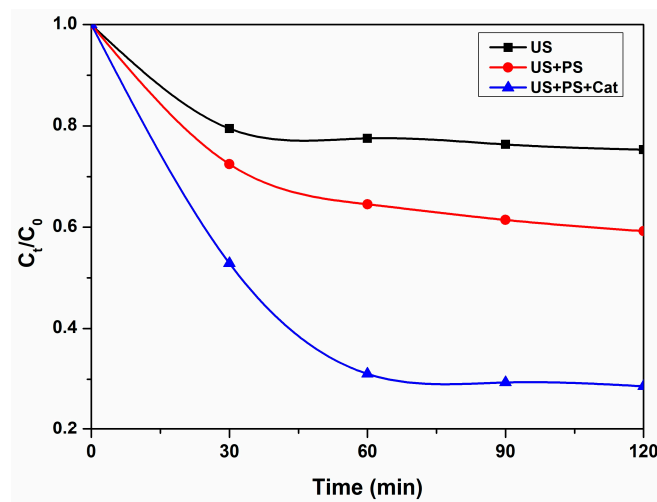
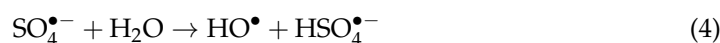
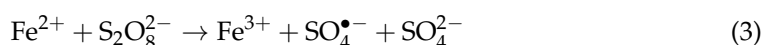


Figure 5. Degradation of dioxane using US, US + PS, and US + PS + Cat.

As a result of sonolysis, catalyst activity may be increased through surface activation, an increase in mass transport, and the breakage of aggregation. One or more of these phenomena can occur alone or in combination [46]. Thus, fruitful oxidation reactions ensured a better degradation effect. In addition, Fe particles in the catalyst facilitated the generation of extra hydroxyl radicals due to acoustic cavitation-induced iron ion transformation from Fe⁰ to Fe²⁺ and Fe³⁺ [47].



Although the quantum of radicals in PS was greater, the lack of fruitful collisions between reactants caused a lesser degree of oxidation. Furthermore, radical scavenging contributed to the imperfect interaction between the reactants. On the other hand, Figure 6 clearly illustrates that the percent degradation of dioxane and the degradation rate was as follows: US < US + PS < US + PS + Cat. Figure 6 also reveals that the reaction order subsequently shifted, which may be attributed to the recombination of radicals, consumption of PS radicals, and mass transfer effects, respectively, in the case of US, US + PS, and US + PS + Cat. It may also result from the shift in radical oxidation mechanisms to non-radical processes [46]. During the initial stages of reaction kinetics, where maximum degradation is observed, the reaction rate constants are 0.0067 min⁻¹, 0.01 min⁻¹, and 0.167 min⁻¹, respectively. The equation for finding the rate constant during the initial stage is presented in Equation (5), where C_A represents the dioxane concentration, K represents the rate constant, and n and t are order and time, respectively.

$$\frac{-dC_A}{dt} = KC_A^n \quad (5)$$

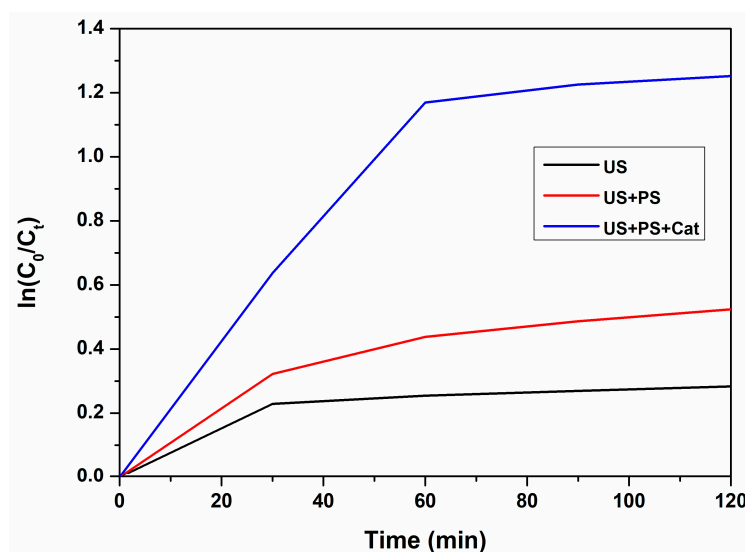


Figure 6. Degradation kinetics of dioxane ($K_{US} < K_{US+PS} < K_{US+PS+Cat}$).

In order to activate PS sonocatalytically, two methods were employed: the single-stage addition of PS and the two-stage addition of PS. In addition to having a catalytic effect on the degradation, Fe interacts directly with sulfate radicals in the reaction [48]. According to Figure 7, the two-stage addition of PS in the presence of FeNP/Z provides a better degradation effect than the single-stage addition. Regarding single-stage PS addition, the excess amount of generated radicals causes the recombination of radicals, resulting in an overall scavenging effect, i.e., an inability to fully utilize the moles of activated oxidant to oxidize the target pollutant. The second-time addition has also been observed to maintain the degradation pathway and ensure it is active and stable, as opposed to single-stage addition, which reaches saturation after a specified period. Thus, our tests suggest that degradation effect is improved by adding oxidizing agents stage by stage to the reaction medium.

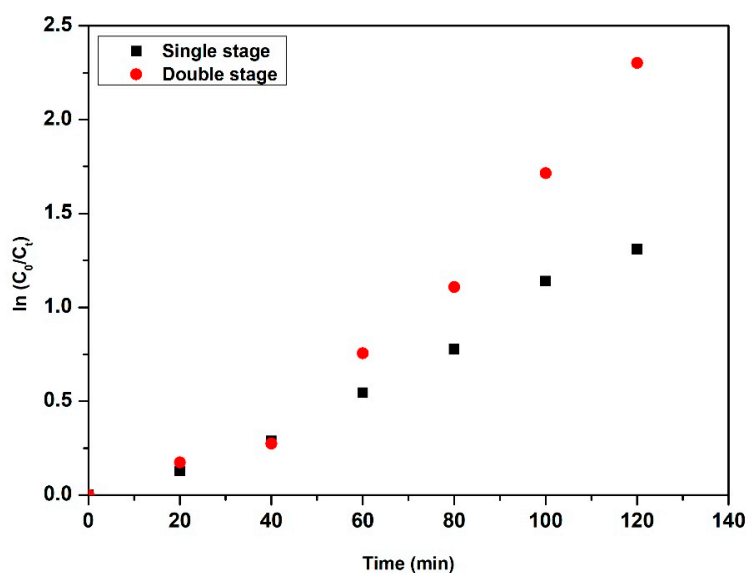


Figure 7. Degradation of dioxane in single and double stages.

2.3. Identification of Reactive Species, Degradation Routes, and Intermediates

Figure 8 illustrates two plausible degradation pathways: one initiated by $\text{HO}\bullet$ and one by $\text{SO}_4^{\bullet-}$. In the presence of various oxidizing radicals and other intermediates, dioxane can undergo a variety of degradation routes. Generally, dioxane undergoes oxidation

through its cyclic structure-opening mechanism. Among its products are aldehydes, ethylene glycol, organic acids, mono- and diformate esters, and oxalate anions [49]. Ultimately, due to degradation, organic carbon is mineralized into carbon dioxide and water [50].

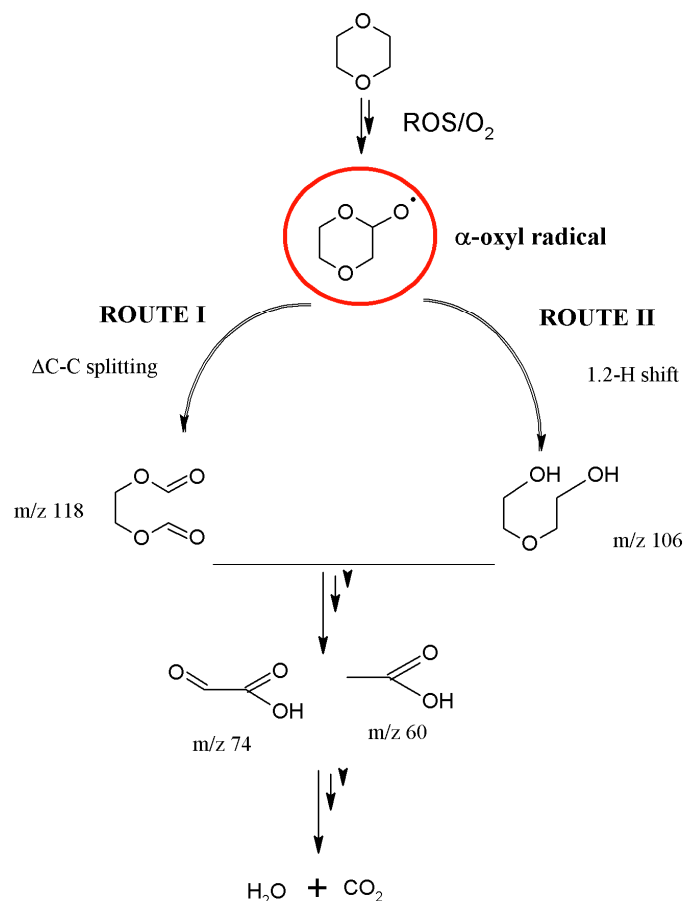


Figure 8. A possible pathway for the degradation of dioxane in the presence of a catalyst.

The tests performed via GC-MS analysis revealed that ethyl glycol (m/z 62), diethyl ester, butanedioic acid, acetic acid (m/z 60), propionic acid, etc., are formed. The opening of the dioxane cyclic structure results in the formation of peroxy radicals via H[•] abstraction [49]. Furthermore, ethylene glycol diformate (EGDF, m/z 118) was also identified, which is formed when the +oxyl radical and hydroxyl radical collide, resulting in glyoxylic acid (m/z 74). Studies have demonstrated that EGDF is one of the major intermediates of dioxane oxidation [21,51]. In the degradation process, diethylene glycol (DEG, m/z 106) is produced by a 1,2-H shift of α-oxyl radicals by SO₄^{•-} radicals, which leads to the formation of acetic acid (m/z 60) [49]. As a result of the pathway, CO₂ and H₂O could be formed, indicating that dioxane was being mineralized.

3. Materials and Methods

3.1. Materials

Dichloromethane (CH₂Cl₂), sodium persulfate (Na₂S₂O₈), methanol, and 1,4-dioxane (C₄H₈O₂) were purchased from POCH, Poland. Tertbutyl alcohol (TBA), Isopropyl alcohol (IPA), and sodium borohydride were purchased from Sigma-Aldrich, Darmstadt, Germany. Iron (III) chloride (FeCl₃, 99%) was purchased from QUALI-TECH INDUSTRIES, SHUNLI, Singapore. The molecular sieve, Siliporite[®], was purchased from Arkema, Colombes, France. Analytical-grade chemicals and solvents were used without further purification. All experiments were conducted using double-deionized water.

3.2. Experimental

3.2.1. Sonochemical Impregnation of Iron Nanoparticles on Molecular Sieves

The molecular sieves were first dispersed in 200 mL of DI water using ultrasonic irradiation for 5 min. A 50 mL solution of 0.1 M FeCl_3 was added to the dispersion and thoroughly mixed via ultrasonic irradiation for another 5 min. Subsequently, FeCl_3 was sonochemically reduced using 0.1 M sodium borohydride solution (100 mL) under ultrasonic irradiation for 1 h in the presence of molecular sieves. Consequently, FeNPs were deposited on molecular sieves. Later, they were thoroughly washed with ethanol, separated via being centrifuged at 5000 rpm for 10 min, and dried in an oven at 60° overnight. The iron nanoparticles deposited on molecular sieves were stored at room temperature in a dry environment for later use. Figure 9 illustrates a schematic representation of the synthesis of the iron nanoparticles that impregnated the molecular sieves.

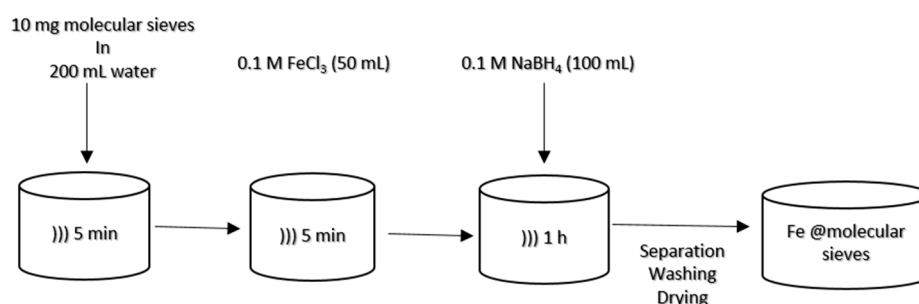


Figure 9. Schematic diagram for FeNP/Z synthesis.

3.2.2. Degradation Studies of Dioxane

The dioxane degradation process was conducted in a Hielscher 400th ultrasonic probe reactor (Hielscher Ultrasonics, Teltow, Germany) with a fixed frequency (24 kHz) and intensity (105 W/cm^2), as shown in Figure 10. In this process, energy is supplied to a transducer, which converts the electrical energy into mechanical vibrations, and attached to an ultrasonic probe. The probe, which was 10 mm in diameter, is stationed, naturally, below the surface of the reacting medium. Typical experimental protocols involve placing a 500 mL solution of 100 ppm dioxane in a steel US reactor. The US phenomena results in a rise in reaction media temperature. Subsequently, the temperature was maintained at $25 \pm 2^\circ \text{C}$ using a refrigerated bath (Chrompack RTE-110B, Neslab Instruments, Forstell, MO, USA). In the beginning of our experiments, the degradation tests were conducted solely using the US effect. In subsequent tests, catalytic, PS, and US effects on dioxane degradation were examined separately. In all experiments, deionized water was used without any pH adjustment.

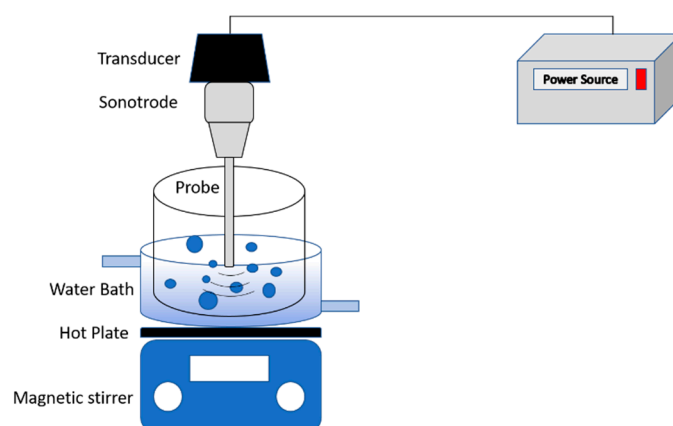


Figure 10. Ultrasonic experimental setup for the degradation of dioxane.

3.3. Process Control and Intermediates Identification by Gas Chromatography

Dioxane was pre-concentrated from water samples prior to analysis via a dispersive liquid-liquid microextraction (DLLME). Obtained extracts were analyzed by employing gas chromatography (a Clarus 580 gas chromatograph and flame ionization detector (GC-FID) from PerkinElmer, Chicago, IL, USA). A detailed description of the procedure can be found in our previous study [52,53]. The identification of intermediates was performed using DLLME followed by gas chromatography coupled with mass spectrometry (DLLME-GC-MS) using a GCMSQP2010SE (Shimadzu, Kyoto, Japan) instrument, following the protocol laid out in an earlier study [44]. The procedure for determining the amount of dioxane was described by Fedorov et al. (2023) [54].

4. Cost Estimation

The energy intensity of the given probe sonicator is 105 W/cm^2 , which requires 82.5 W of electrical energy input into the system for the 10 mm probe. The energy calculations are calculated by using 1 m^3 of dioxane polluted wastewater volume as the basis:

$$\text{Reaction volume} = 500 \text{ mL}$$

$$\text{Energy input} = 82.5 \text{ W}$$

$$\text{Input electrical energy required per } 1 \text{ m}^3 \text{ of wastewater} = 82.5 \text{ W} / 0.5 \text{ l} = 165 \text{ kW/m}^3$$

$$\text{Total power consumption} = \text{Input energy} * \text{time of sonication} = 330 \text{ kWh/m}^3$$

Total cost of operation = Total power consumption * Cost per unit electricity (Avg. cost of unit electricity is INR 6 [as per Northern Power Distribution Company of Telangana State electricity prices]).

For US alone:

$$\text{Total cost} = 330 \text{ kWh/m}^3 * 6 \text{ INR/kWh} = 1980 \text{ INR/m}^3 \text{ of wastewater treatment}$$

For US + PS

$$\text{Total cost} = 1980 \text{ INR/m}^3 + \text{Cost of PS (R}_{\text{ox}} = 2) \text{ per m}^3 \text{ of wastewater (75 INR/m}^3) \text{ [Avg. wholesale price of sodium persulfate (Technical Grade) is INR 130/kg (Antares Chem Pvt Ltd., Mumbai, MS, India)]} = 2055 \text{ INR/m}^3$$

For US + PS + Cat

$$\text{Total cost} = 1980 \text{ INR/m}^3 + 75 \text{ INR/m}^3 + \text{cost of doping for the preparation of } 5 \text{ mg catalyst}$$

Time of ultrasonication of doping is 1 h for 1 g of composite catalyst preparation. Hence, the price is INR 0.85 per 5 mg catalyst [Avg. wholesale cost of zeolite is INR 280/kg and considering other chemical cost].

Hence, the total cost to treat 1 m^3 of 100 mg/L concentration of dioxane wastewater is approximately INR 3755.

5. Conclusions

For the current study, we investigated whether doping FeNPs on zeolite and the sonocatalytic activation of PS had an effect on the degradation of dioxane. Zeolite was successfully doped with FeNPs by using ultrasonication, and a composite catalyst with improved characteristics was developed. Sonolytically activated PS in the presence of FeNP/Z was studied to determine the degradation of dioxane. It yielded a significant synergistic effect on dioxane degradation. The catalyst enhanced the degradation rate and reduced the quantity of PS required for complete degradation. Further, through the use of GC-MS analysis, the degradation pathways were proposed. Our experiments revealed that dioxane degradation can be achieved by opening its cyclic structure. The opening of the structure occurs due to $\Delta\text{C-C}$ splitting or $1,2\text{-H}$ shift. Finally, the estimated cost of

dioxane degradation using our proposed methodology was reported. As demonstrated in the present study, the combination of US and a catalyst synergistically activates PS and phenomenally enhances the rate and effects of degradation.

Author Contributions: Conceptualization, S.H.S. and G.B.; Formal analysis, M.P.R. and J.K.; Investigation, S.T.M. and S.H.S.; Methodology, S.H.S. and G.B.; Resources, G.B.; Supervision, S.H.S. and G.B.; Validation, M.P.R., S.M. and G.B.; Writing—original draft, S.T.M., S.H.S. and M.M.S.; Writing—review and editing, S.T.M., M.M.S., S.M. and G.B. All authors have read and agreed to the published version of the manuscript.

Funding: This research was partially funded by the Ulam Program of Polish National Agency for Academic Exchange, grant number PPN/ULM/2020/1/00037/U/00001” and “National Science Centre, Warsaw, Poland, UMO-2017/25/B/ST8/01364”.

Data Availability Statement: Data available in a publicly accessible repository.

Acknowledgments: Shirish H. Sonawane acknowledges the support from the Ulam program of the Polish National Agency for Academic Exchange (NAWA) (Grant number: PPN/ULM/2020/1/00037/U/00001). The authors gratefully acknowledge the financial support they received from the National Science Centre, Warsaw, Poland, for project OPUS nr UMO-2017/25/B/ST8/01364.

Conflicts of Interest: The authors declare no conflict of interest.

References

1. Geissen, V.; Mol, H.; Klumpp, E.; Umlauf, G.; Nadal, M.; van der Ploeg, M.; van de Zee, S.E.A.T.M.; Ritsema, C.J. Emerging pollutants in the environment: A challenge for water resource management. *Int. Soil Water Conserv. Res.* **2015**, *3*, 57–65. [[CrossRef](#)]
2. Ghumra, D.P.; Agarkoti, C.; Gogate, P.R. Improvements in effluent treatment technologies in Common Effluent Treatment Plants (CETPs): Review and recent advances. *Process Saf. Environ. Prot.* **2021**, *147*, 1018–1051. [[CrossRef](#)]
3. Malkapuram, S.T.; Sharma, V.; Gumfekar, S.P.; Sonawane, S.; Sonawane, S.; Boczkaj, G.; Seepana, M.M. A review on recent advances in the application of biosurfactants in wastewater treatment. *Sustain. Energy Technol. Assess.* **2021**, *48*, 101576. [[CrossRef](#)]
4. Kumari, S.; Debnath, M.; Sonawane, S.H.; Malkapuram, S.T.; Seepana, M.M. Dye Decolorization by *Rhodococcus ruber* Strain TES III Isolated from Textile Effluent Wastewater Contaminated Soil. *ChemistrySelect* **2022**, *7*, e202200421. [[CrossRef](#)]
5. Salimi, M.; Esrafil, A.; Gholami, M.; Jafari, A.J.; Kalantary, R.R.; Farzadkia, M.; Kermani, M.; Sobhi, H.R. Contaminants of emerging concern: A review of new approach in AOP technologies. *Environ. Monit. Assess.* **2017**, *189*. [[CrossRef](#)]
6. Kim, S.; Chu, K.H.; Al-Hamadani, Y.A.J.; Park, C.M.; Jang, M.; Kim, D.H.; Yu, M.; Heo, J.; Yoon, Y. Removal of contaminants of emerging concern by membranes in water and wastewater: A review. *Chem. Eng. J.* **2018**, *335*, 896–914. [[CrossRef](#)]
7. Joseph, L.; Jun, B.M.; Jang, M.; Park, C.M.; Muñoz-Senmache, J.C.; Hernández-Maldonado, A.J.; Heyden, A.; Yu, M.; Yoon, Y. Removal of contaminants of emerging concern by metal-organic framework nano-adsorbents: A review. *Chem. Eng. J.* **2019**, *369*, 928–946. [[CrossRef](#)]
8. Zhu, J.; Li, B. Degradation Kinetic and Remediation Effectiveness of 1,4-Dioxane-Contaminated Groundwater by a Sono-Activated Persulfate Process. *J. Environ. Eng.* **2018**, *144*, 1–8. [[CrossRef](#)]
9. Klečka, G.M.; Gonsior, S.J. Removal of 1,4-dioxane from wastewater. *J. Hazard. Mater.* **1986**, *13*, 161–168. [[CrossRef](#)]
10. Stepien, D.K.; Diehl, P.; Helm, J.; Thoms, A.; Püttmann, W. Fate of 1,4-dioxane in the aquatic environment: From sewage to drinking water. *Water Res.* **2014**, *48*, 406–419. [[CrossRef](#)]
11. Doherty, A.-C.; Lee, C.-S.; Meng, Q.; Sakano, Y.; Noble, A.E.; Grant, K.A.; Esposito, A.; Gobler, C.J.; Venkatesan, A.K. Contribution of household and personal care products to 1,4-dioxane contamination of drinking water. *Curr. Opin. Environ. Sci. Health* **2023**, *31*, 100414. [[CrossRef](#)]
12. Vatankhah, H.; Szczuka, A.; Mitch, W.A.; Almaraz, N.; Brannum, J.; Bellona, C. Evaluation of Enhanced Ozone-Biologically Active Filtration Treatment for the Removal of 1,4-Dioxane and Disinfection Byproduct Precursors from Wastewater Effluent. *Environ. Sci. Technol.* **2019**, *53*, 2720–2730. [[CrossRef](#)] [[PubMed](#)]
13. Nawaz, T.; Sengupta, S. Contaminants of Emerging Concern: Occurrence, Fate, and Remediation. In *Advances in Water Purification Techniques*; Elsevier: Amsterdam, The Netherlands, 2019; pp. 67–114. [[CrossRef](#)]
14. Ghatak, H.R. Advanced Oxidation Processes for the Treatment of Biorecalcitrant Organics in Wastewater. *Crit. Rev. Environ. Sci. Technol.* **2014**, *44*, 1167–1219. [[CrossRef](#)]
15. Miklos, D.B.; Remy, C.; Jekel, M.; Linden, K.G.; Hübner, U. Evaluation of advanced oxidation processes for water and wastewater treatment—A critical review. *Water Res.* **2018**, *139*, 118–131. [[CrossRef](#)]
16. Xu, X.; Zhong, Y.; Shao, Z. Double Perovskites in Catalysis, Electrocatalysis, and Photo(electro)catalysis. *Trends Chem.* **2019**, *1*, 410–424. [[CrossRef](#)]
17. Krishnan, S.; Rawindran, H.; Sinnathambi, C.M.; Lim, J.W. Comparison of various advanced oxidation processes used in remediation of industrial wastewater laden with recalcitrant pollutants. *IOP Conf. Ser. Mater. Sci. Eng.* **2017**, *206*. [[CrossRef](#)]

18. Dong, H.; Zeng, G.; Tang, L.; Fan, C.; Zhang, C.; He, X.; He, Y. An overview on limitations of TiO₂-based particles for photocatalytic degradation of organic pollutants and the corresponding countermeasures. *Water Res.* **2015**, *79*, 128–146. [[CrossRef](#)]
19. Trellu, C.; Chaplin, B.P.; Coetsier, C.; Esmilaire, R.; Cerneaux, S.; Causserand, C.; Cretin, M. Electro-oxidation of organic pollutants by reactive electrochemical membranes. *Chemosphere* **2018**, *208*, 159–175. [[CrossRef](#)]
20. Barisci, S.; Suri, R. Degradation of 4-dioxane from water and plating industry wastewater using electrochemical batch and plug flow reactors. *J. Appl. Electrochem.* **2022**, *53*, 1169–1181. [[CrossRef](#)]
21. Byrne, C.; Dervin, S.; Hermosilla, D.; Merayo, N.; Blanco, Á.; Hinder, S.; Harb, M.; Dionysiou, D.D.; Pillai, S.C. Solar light assisted photocatalytic degradation of 1,4-dioxane using high temperature stable anatase W-TiO₂ nanocomposites. *Catal. Today* **2021**, *380*, 199–208. [[CrossRef](#)]
22. Vikas, S.S.S.S.; Ghodke, S.; Teja, S.; Dilipkumar, P.; Sonawane, S.H.; Gaikwad, R. Ultrasonication based wastewater treatment. In *Novel Approaches towards Wastewater Treatment and Resource Recovery*; Elsevier: Amsterdam, The Netherlands, 2022; pp. 221–240. [[CrossRef](#)]
23. Gogate, P.R.; Pandit, A.B. A review of imperative technologies for wastewater treatment II: Hybrid methods. *Adv. Environ. Res.* **2004**, *8*, 553–597. [[CrossRef](#)]
24. Taylor, P.; Wang, J.L.; Xu, L.J. Advanced Oxidation Processes for Wastewater Treatment: Formation of Hydroxyl Radical and Application. *Crit. Rev. Environ. Sci. Technol.* **2011**, *42*, 37–41. [[CrossRef](#)]
25. Xu, Z.; Mochida, K.; Naito, T.; Yasuda, K. Effects of operational conditions on 1,4-Dioxane degradation by combined use of ultrasound and ozone microbubbles. *Jpn. J. Appl. Phys.* **2012**, *51*, 07GD08. [[CrossRef](#)]
26. Yang, L.; Xue, J.; He, L.; Wu, L.; Ma, Y.; Chen, H.; Li, H.; Peng, P.; Zhang, Z. Review on ultrasound assisted persulfate degradation of organic contaminants in wastewater: Influences, mechanisms and prospective. *Chem. Eng. J.* **2019**, *378*, 122146. [[CrossRef](#)]
27. Sonawane, S.; Rayaroth, M.P.; Landge, V.K.; Fedorov, K.; Boczkaj, G. Thermally activated persulfate-based Advanced Oxidation Processes—Recent progress and challenges in mineralization of persistent organic chemicals: A review. *Curr. Opin. Chem. Eng.* **2022**, *37*, 100839. [[CrossRef](#)]
28. Panda, D.; Saharan, V.K.; Manickam, S. Controlled hydrodynamic cavitation: A review of recent advances and perspectives for greener processing. *Processes* **2020**, *8*, 220. [[CrossRef](#)]
29. Waclawek, S.; Lutze, H.V.; Grübel, K.; Padil, V.V.T.; Černík, M.; Dionysiou, D.D. Chemistry of persulfates in water and wastewater treatment: A review. *Chem. Eng. J.* **2017**, *330*, 44–62. [[CrossRef](#)]
30. Fagan, W.P.; Zhao, J.; Villamena, F.A.; Zweier, J.L.; Weavers, L.K. Synergistic, aqueous PAH degradation by ultrasonically-activated persulfate depends on bulk temperature and physicochemical parameters. *Ultrason. Sonochem.* **2020**, *67*, 105172. [[CrossRef](#)]
31. Yang, L.; Jiao, Y.; Xu, X.; Pan, Y.; Su, C.; Duan, X.; Sun, H.; Liu, S.; Wang, S.; Shao, Z. Superstructures with Atomic-Level Arranged Perovskite and Oxide Layers for Advanced Oxidation with an Enhanced Non-Free Radical Pathway. *ACS Sustain. Chem. Eng.* **2022**, *10*, 1899–1909. [[CrossRef](#)]
32. Deng, J.; Feng, S.F.; Zhang, K.; Li, J.; Wang, H.; Zhang, T.; Ma, X. Heterogeneous activation of peroxymonosulfate using ordered mesoporous Co₃O₄ for the degradation of chloramphenicol at neutral pH. *Chem. Eng. J.* **2017**, *308*, 505–515. [[CrossRef](#)]
33. Hu, Y.; He, Y.; Wang, X.; Wei, C. Efficient adsorption of phenanthrene by simply synthesized hydrophobic MCM-41 molecular sieves. *Appl. Surf. Sci.* **2014**, *311*, 825–830. [[CrossRef](#)]
34. Karataev, O.R.; Novikov, V.F.; Karataeva, E.S.; Kartashova, A.A. Use of modified molecular sieves in mechanical filters. *IOP Conf. Ser. Mater. Sci. Eng.* **2019**, *570*, 11–14. [[CrossRef](#)]
35. Wu, M.; Deng, H.; Shi, J.; Wang, Z. Transition element doped octahedral manganese molecular sieves (Me-OMS-2) as diclofenac adsorbents. *Chemosphere* **2020**, *258*, 127120. [[CrossRef](#)]
36. Leal, T.W.; Lourenço, L.A.; de L. Brandão, H.; da Silva, A.; de Souza, S.M.A.G.U.; de Souza, A.A.U. Low-cost iron-doped catalyst for phenol degradation by heterogeneous Fenton. *J. Hazard. Mater.* **2018**, *359*, 96–103. [[CrossRef](#)]
37. Ruiz-Baltazar, A.; Esparza, R.; Gonzalez, M.; Rosas, G.; Pérez, R. Preparation and characterization of natural zeolite modified with iron nanoparticles. *J. Nanomater.* **2015**, *2015*, 364763. [[CrossRef](#)]
38. Vasconcellos, C.M.; Gonçalves, M.L.A.; Pereira, M.M.; Carvalho, N.M.F. Iron doped manganese oxide octahedral molecular sieve as potential catalyst for SO_x removal at FCC. *Appl. Catal. A Gen.* **2015**, *498*, 69–75. [[CrossRef](#)]
39. Guaya, D.; Jiménez, R.; Sarango, J.; Valderrama, C.; Cortina, J.L. Iron-doped natural clays: Low-cost inorganic adsorbents for phosphate recovering from simulated urban treated wastewater. *J. Water Process Eng.* **2021**, *43*. [[CrossRef](#)]
40. Wang, H.; Li, X.; Meng, F.; Wang, G.; Zhang, D. Preparation and evaluation of iron nanoparticles embedded CNTs grown on ZSM-5 as catalysts for NO decomposition. *Chem. Eng. J.* **2020**, *392*, 123798. [[CrossRef](#)]
41. Chen, C.; Yang, X.-D.; Zhou, Z.-Y.; Lai, Y.-J.; Rauf, M.; Wang, Y.; Pan, J.; Zhuang, L.; Wang, Q.; Wang, Y.-C.; et al. Aminothiazole-derived N,S,Fe-doped graphene nanosheets as high performance electrocatalysts for oxygen reduction. *Chem. Commun.* **2015**, *51*, 17092–17095. [[CrossRef](#)]
42. Xiao, S.; Cheng, M.; Zhong, H.; Liu, Z.; Liu, Y.; Yang, X.; Liang, Q. Iron-mediated activation of persulfate and peroxymonosulfate in both homogeneous and heterogeneous ways: A review. *Chem. Eng. J.* **2020**, *384*, 123265. [[CrossRef](#)]
43. Ramakrishna, C.; Krishna, R.; Gopi, T.; Swetha, G.; Saini, B.; Shekar, S.C.; Srivastava, A. Complete oxidation of 1,4-dioxane over zeolite-13X-supported Fe catalysts in the presence of air. *Cuihua Xuebao/Chin. J. Catal.* **2016**, *37*, 240–249. [[CrossRef](#)]
44. Sonawane, S.; Fedorov, K.; Rayaroth, M.P.; Boczkaj, G. Degradation of 4-dioxane by sono-activated persulfates for water and wastewater treatment applications. *Water Resour. Ind.* **2022**, *28*, 100183. [[CrossRef](#)]

45. Entezari, M.H.; Heshmati, A.; Sarafraz-Yazdi, A. A combination of ultrasound and inorganic catalyst: Removal of 2-chlorophenol from aqueous solution. *Ultrason. Sonochem.* **2005**, *12*, 137–141. [[CrossRef](#)]
46. Chen, N.; Lee, D.; Kang, H.; Cha, D.; Lee, J.; Lee, C. Catalytic persulfate activation for oxidation of organic pollutants: A critical review on mechanisms and controversies. *J. Environ. Chem. Eng.* **2022**, *10*, 107654. [[CrossRef](#)]
47. Zhao, L.; Hou, H.; Fujii, A.; Hosomi, M.; Li, F. Degradation of 1,4-dioxane in water with heat- and Fe²⁺-activated persulfate oxidation. *Environ. Sci. Pollut. Res.* **2014**, *21*, 7457–7465. [[CrossRef](#)] [[PubMed](#)]
48. Li, Z.-Y.; Wang, L.; Liu, Y.-L.; Zhao, Q.; Ma, J. Unraveling the interaction of hydroxylamine and Fe(III) in Fe(II)/Persulfate system: A kinetic and simulating study. *Water Res.* **2020**, *168*, 115093. [[CrossRef](#)]
49. Tawfik, A. Degradation pathways of 1,4-dioxane in biological and advanced oxidation processes. *Desalin. Water Treat.* **2020**, *178*, 360–386. [[CrossRef](#)]
50. Beckett, M.A.; Hua, I. Elucidation of the 1,4-dioxane decomposition pathway at discrete ultrasonic frequencies. *Environ. Sci. Technol.* **2000**, *34*, 3944–3953. [[CrossRef](#)]
51. Beckett, M.A.; Hua, I. Enhanced sonochemical decomposition of 1,4-dioxane by ferrous iron. *Water Res.* **2003**, *37*, 2372–2376. [[CrossRef](#)]
52. Boczkaj, G.; Makoś, P.; Przyjazny, A. Application of dispersive liquid-liquid microextraction and gas chromatography with mass spectrometry for the determination of oxygenated volatile organic compounds in effluents from the production of petroleum bitumen. *J. Sep. Sci.* **2016**, *39*, 2604–2615. [[CrossRef](#)]
53. Makoś, P.; Fernandes, A.; Boczkaj, G. Method for the simultaneous determination of monoaromatic and polycyclic aromatic hydrocarbons in industrial effluents using dispersive liquid-liquid microextraction with gas chromatography-mass spectrometry. *J. Sep. Sci.* **2018**, *41*, 2360–2367. [[CrossRef](#)] [[PubMed](#)]
54. Fedorov, K.; Plata-Gryl, M.; Khan, J.A.; Boczkaj, G. Ultrasound-assisted heterogeneous activation of persulfate and peroxymonosulfate by asphaltenes for the degradation of BTEX in water. *J. Hazard. Mater.* **2020**, *397*, 122804. [[CrossRef](#)] [[PubMed](#)]

Disclaimer/Publisher's Note: The statements, opinions and data contained in all publications are solely those of the individual author(s) and contributor(s) and not of MDPI and/or the editor(s). MDPI and/or the editor(s) disclaim responsibility for any injury to people or property resulting from any ideas, methods, instructions or products referred to in the content.

